Spinodal instability in an expanding universe

Author: Pau Pagès Gutiérrez
Facultat de Física, Universitat de Barcelona, Diagonal 645, 08028 Barcelona, Spain.

Advisor: Jorge Casaderrey Solana

We study the dynamics of matter undergoing a first order phase transition in an expanding universe. We contemplate the scenario where the universe experiences significant supercooling, leading to local instability known as spinodal instability. We use second-order hydrodynamics to derive the equation that governs the behavior of the unstable modes that arise in this situation, and numerically solve it. The resulting solutions differ significantly from the ones found for a flat universe. Specifically, we observe a damped behaviour and a notable time dependence in the momentum range of the unstable modes, highlighting the richer dynamics at play. Finally, we model this time dependence using an adiabatic approximation and show that it captures the main momentum and expansion rate dependence of unstable modes growth.

I. INTRODUCTION

In the field of cosmology, one of the intriguing aspects of the early universe is the occurrence of phase transitions. These transitions involve changes in the fundamental properties of matter. While the standard model does not posses a first-order phase transition, many of its extensions show such behaviour. If that is the case, the early universe can probe the dynamics of the transitions as it cools and expands [1]. Such phase transitions in the early universe are known to generate gravitational waves that have the potential to be detected in forthcoming experiments like the LISA mission.

A precise understanding of the dynamics involved in the phase transition may be crucial in the discovery process. Conventionally, the phase transition is believed to occur through the nucleation of bubbles, where the stable phase forms within the metastable phase that has been supercooled. However, it has been observed [2, 3] that under certain conditions the nucleation rate may be sufficiently suppressed enabling the universe to continue to supercool until reaching the end of the metastable branch (for further details, refer to Sec. 3.1 in [2]). In such conditions, the universe eventually enters the spinodal region (FIG. 1), and the transition progresses through the exponential growth of unstable modes and subsequent formation, merging, and relaxation of phase domains [3].

FIG. 1 shows the different phases the early universe can undergo. States lying along the red dashed-dotted curve are thermodynamically unstable due to their negative specific heat. In this situation, the primary perturbations that arise are in the form of sound modes with an imaginary speed of sound, while other perturbations, such as those originating from diffusion, can be neglected. Therefore, the dynamics of these states will be studied by examining the behavior of their sound modes. The spinodal instability is well known in the case of a static universe [2–5]. The study considering an expanding universe has yet to be done. Within this context, the aim of this work is to study the behaviour of states in the spinodal region for a dynamical geometry.

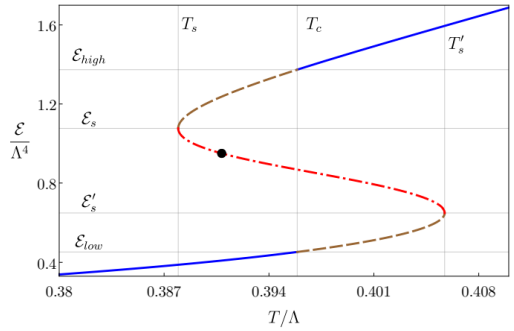

FIG. 1: Energy density as a function of temperature of a typical first-order phase transition. The thermodynamically stable states are represented by the solid, blue curves. The metastable states are depicted by the dashed, brown curves. The unstable states are indicated by the dashed-dotted, red curve. Λ is the characteristic energy scale of the system. (Figure taken from [2]).

In Sec. II, we provide a derivation of the equation governing the sound modes using second-order hydrodynamics. Subsequently, in Sec. III, we numerically solve these equations using the RK4 method and analyze the results in three distinct contexts. First, we assume the universe to be flat and determine the analytical behaviour of the unstable modes. Secondly, by setting a constant speed of sound, $|c_s| = 1/\sqrt{30}$, we gain a comprehensive understanding of the equation and its deviations from the case of a static universe. Finally, we explore a variable speed of sound, which, as we will argue, better approximates the dynamics of overcooled matter in the vicinity of the spinodal transition.

II. DYNAMICS OF SOUND MODES IN DE-SITTER

De-Sitter space (dS) is a theoretical framework that effectively captures the expansion characteristic of the

early universe. With our choice of coordinates, its line element is

$$ds^2 = -dt^2 + e^{2Ht} dx_i dx^i. \tag{1}$$

The curvature of dS is set by the parameter H, which is its intrinsic Hubble constant.

Let us assume an expanding universe, modeled by dS, containing a viscous fluid. Its stress-tensor reads

$$T^{\mu\nu} = \epsilon u^\mu u^\nu + \Delta^{\mu\nu} p + \Pi^{\mu\nu}, \tag{2}$$

where $\Delta^{\mu\nu} p = g^{\mu\nu} + u^\mu u^\nu$ serves as a projection operator on the space orthogonal to the fluid velocity, and $g^{\mu\nu}$ is the metric defined in eq.(1). The viscous stress tensor $\Pi^{\mu\nu}$, which plays a crucial role in characterizing the effects of viscosity, can be determined using second-order hydrodynamics [5, 6].

The conservation of the stress tensor yields

$$\begin{aligned} &D\epsilon + (\epsilon + p)\,\nabla_\mu u^\mu - \Pi^{\mu\nu}\nabla^\perp_{(\mu} u_{\nu)} = 0 \\ &(\epsilon + p)\, Du^\alpha + \nabla^\alpha_\perp p + \Delta^\alpha_\nu \nabla_\mu \Pi^{\mu\nu} = 0. \end{aligned} \tag{3}$$

Here the $(.\ .\ .)$ denote symmetrization and we have introduced the shorthand notations $D \equiv u^\mu \nabla_\mu$ and $\nabla^\alpha_\perp \equiv \Delta^{\mu\alpha}\nabla_\mu$ for the projection of derivatives parallel and perpendicular to u^μ respectively.

Consider small perturbations of energy density and fluid velocity in a system that is initially in equilibrium and at rest. Due to the isotropy of the fluid, we can choose both the momentum k and the velocity u to align with the x-direction. As a result, the perturbation only depends on a single spatial coordinate. In what follows, we will work in the local rest frame, $u^\mu = (1, \mathbf{0})$ so we can focus on the relevant dynamics and properties of the states without considering the effects of fluid motion. We can obtain the equations that describe the sound modes by introducing this perturbations into eqs.(3),

$$\begin{aligned} \partial_t \delta\epsilon + (\epsilon + p)\,\partial_x \delta u^x &= 0 \\ (\epsilon + p)\,(\partial_t \delta u^x + H \delta u^x) + e^{-2Ht}\partial_x \delta p + \nabla_\mu \delta\Pi^{\mu x} &= 0. \end{aligned} \tag{4}$$

Considering a system without conserved charges, all momentum is due to the flow of energy density, i.e. $u^\mu T^{\mu\nu} = \epsilon u^\nu \implies u_\mu \Pi^{\mu\nu} = 0$. This condition implies $\delta\Pi^{0\nu} = 0$. Hence the only not-vanishing term of the viscous stress tensor that contributes in eqs.(4) is $\delta\Pi^{xx}$, which can be written in terms of second-order gradients and reads

$$\delta\Pi^{xx} = -(\epsilon + p)\Gamma_{dS}(H) e^{-2Ht}\partial_x \delta u^x + f_L e^{-4Ht}\partial_x^2 \delta\epsilon. \tag{5}$$

We can write the sound attenuation in de-Sitter space, Γ_{dS}, and the longitudinal transport coefficient, f_L, in terms of the shear and bulk viscosity coefficients, η and ζ respectively, and other second order transport coefficients as

$$\begin{aligned} \Gamma_{dS}(H) = \frac{4}{3}\frac{\eta}{\epsilon + p}\left[1 + \left(\tau_\pi - \frac{\tau^*_\pi}{3}\right) H\right] \\ + \frac{\zeta}{\epsilon + p}\left[1 + \left(\tau_\Pi - 2\tau^*_\Pi\right) H\right] \end{aligned} \tag{6}$$

$$f_L = -\frac{c_s^2}{\epsilon + p}\left(\frac{4}{3}\eta\tau_\pi + \zeta\tau_\Pi\right). \tag{7}$$

The proof of eq.(5), as well as the derivation of both coefficients, can be found in the Appendix.

We can solve eqs.(4) using a spatial Fourier ansatz: $\delta\epsilon = e^{ikx}\delta\epsilon_k(t)$ and $\delta u^i = e^{ikx}\delta u^i_k(t)$. In this representation, x is a comoving coordinate. And, since the physical wavelength of this modes grows in time as $k^{-1}_{phys} = e^{Ht}k^{-1}$ due to the universe expansion, k is not the physical momentum but a mathematical parameter that represents the initial momentum of the mode. In terms of the Fourier components, eqs.(4) become

$$\partial_t \delta\epsilon_k + ik(\epsilon + p)\delta u^x_k = 0 \tag{8}$$

$$\begin{aligned} &(\epsilon + p)\left[\partial_t \delta u^x_k + H\delta u^x_k\right] + ike^{-2Ht}c_s^2\delta\epsilon_k \\ &\quad + k^2(\epsilon + p)e^{-2Ht}\Gamma\delta u^x_k - ik^3 f_L e^{-4Ht}\delta\epsilon_k = 0, \end{aligned} \tag{9}$$

where we have used the state equation to compute the pressure gradient as $\partial_x p = (dp/d\epsilon)\partial_x\epsilon = c_s^2\partial_x\epsilon$.

From the continuity equation in dS (first equation in eqs.(3)) one knows the behaviour of the background energy. In the local rest frame $D \longrightarrow \partial_t$, $\nabla_\mu u^\mu = \partial_\mu u^\mu + \Gamma^\mu_{\mu\rho}u^\rho = \Gamma^i_{i0}u^0 = H$ and $\nabla^\perp_{(\mu}u_{\nu)} = 0$. Then $\partial_t\epsilon = -H(\epsilon + p)$. Combining eq.(8) and (9) and using this result, one finds that the energy density perturbations for a viscous fluid in an expanding universe behave following a differential equation that reads

$$\begin{aligned} \partial_t^2\delta\epsilon_k + \left(k^2e^{-2Ht}\Gamma_{dS}(H) + (2 + c_s^2)H\right)\partial_t\delta\epsilon_k \\ + k^2e^{-2Ht}\left(c_s^2 - k^2e^{-2Ht}f_L\right)\delta\epsilon_k = 0. \end{aligned} \tag{10}$$

In the limit of Minkowski space ($H \to 0$), we recover the sound mode equations for a static universe, which can be found in the appendix section of [3]. However, in the presence of a non-zero Hubble parameter, we need to pay extra attention to the term $(2 + c_s^2)H$, which acts like a viscosity arising from the expansion of the universe. It is important to note that this term only acts as a viscosity when $|c_s^2| < 2$, which is satisfied in our study cases as discussed in Sec. III C. Based on this, we can already deduce that the perturbations will exhibit a damped behavior compared to the Minkowski case.

III. SPINODAL INSTABILITY

A. Spinodal instability in flat space

In order to validate the numerical procedure, we will also simulate the Minkowski case with a constant speed

of sound, as it has an analytical solution. The speed of sound is defined by $c_s^2 \equiv dP/d\epsilon = s/c_v$, where s is the entropy density, and c_v is the specific heat. In the spinodal region c_v is negative and, since the entropy density is positive everywhere, c_s^2 is also negative and hence, c_s imaginary. In order to study states that are located near the spinodal point, we set the value of sound speed to be small, $|c_s| = 1/\sqrt{30}$.

In this context, setting $H = 0$ in eq.(10) provides a solution that is also documented in [2, 3]. This solution yields the following growth rate, up to second order in momentum, for the unstable modes,

$$\gamma(k) = k|c_s| - \frac{k^2}{2}\Gamma. \tag{11}$$

We observe that the perturbations will only grow for momenta in the range $0 < k < k_* = \frac{2|c_s|}{\Gamma} \approx 1.38T$. The numerical values used for Γ are discussed in Sec. III B. The spinodal instability exhibits an infrared nature, indicating that only modes with momentum below a specific threshold are susceptible to instability. The most unstable mode, corresponding to the mode with the largest growth rate, has momentum given by $k_{\max} = \frac{|c_s|}{\Gamma} \approx 0.69T$. We will use these results to verify the accuracy of our numerical calculations. Furthermore, since the unstable modes dominate the dynamics of the system, and since their typical momentum is $k \lesssim T$, we conclude that hydrodynamics is a valid approximation.

B. Spinodal instability in de-Sitter with fixed sound speed

Before analyzing the real physical situation, let us begin by considering a simpler case with constant sound speed, in specific $|c_s| = 1/\sqrt{30}$. This choice will let us compare the dynamics in dS and in Minkowski space.

Unlike the flat universe case, eq.(10) is not analytically solvable and numerical methods are required. The computations were performed in Fortran using the RK4 method. In order to carry out these computations, we treated the temperature as an independent parameter and expressed all other variables in terms of it. The choice of viscosity coefficients was based on existing literature, specifically references such as [2, 3, 7]. Briefly, we set $\Gamma_{dS}(t = t_s) = \Gamma = \frac{5}{6\pi}$ and $f_L = -\Gamma_{dS}^2/4$ where t_s represents the time at which the perturbation forms at the spinodal point. However, it is important to note that in the de-Sitter space, these coefficients will have a dependence on time, given by $\sim e^{H(t-t_s)}$, due to the thermal variation induced by the universe expansion. In addition, it is worth noting that the growth of unstable modes will be more pronounced for smaller values of H, as the expansion of the universe acts as a damping viscosity on the perturbations. To ensure that our study differs significantly from the case of a static universe while still allowing for analysis of important unstable modes, we set $H = 0.01T$. Other values of H will be explored in Sec. III C. Moreover, all the computations have been made assuming an initial amplitude of $0.1T$.

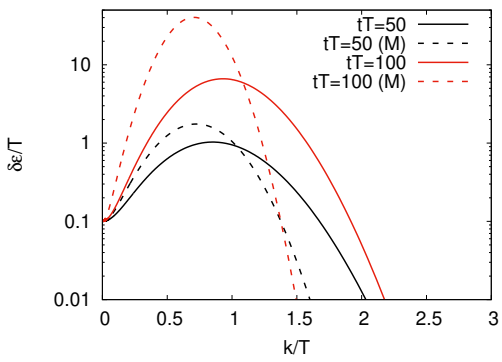

FIG. 2: Perturbations energy as a function of the mode's momentum for different times ($tT = 50$ indicated in black and $tT = 100$ indicated in red) and for both the Minkowski (dashed curves) and de-Sitter (solid curves) cases.

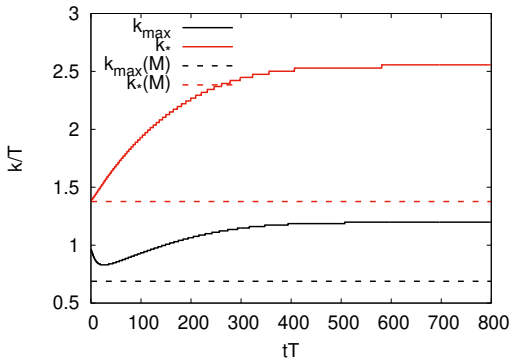

FIG. 3: Maximum mode (shown in black) and the threshold mode (shown in red) as functions of the time for for both the Minkowski (dashed curves) and de-Sitter (solid curves) cases.

FIG. 2 shows the behaviour of the perturbation for different modes in both the dS and Minkowski cases. The numerical results in the Minkowski case align with the anticipated values, providing confirmation of the validity of the computations. Regarding the results in dS, we observe that they exhibit a damped behavior compared to the static universe case, as predicted earlier. Furthermore, both the most unstable mode and the threshold shift to larger momenta as time progresses.

The complete time evolution of these modes is depicted in FIG. 3, in which we recognize that the perturbations become frozen after a certain amount of time has passed. This freezing behavior can be deduced from eq.(13) in the limit of large times by introducing the variable transformation $\tau = e^{-Ht}$. One obtains a power series solution in terms of τ, and in the limit of large times, only the zeroth-order term remains. This term is a constant that depends on k and H. This serves as a further test for our numerical results.

It is important to note that, unlike the Minkowski case,

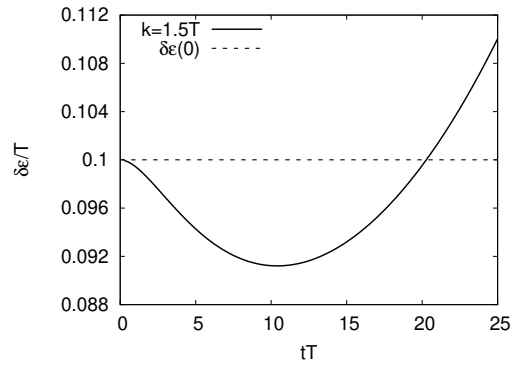

FIG. 4: Perturbation's behaviour for a mode with momentum $k > k_*(0)$. The value $\delta\epsilon(0)$ has also been illustrated by a dotted grey curve.

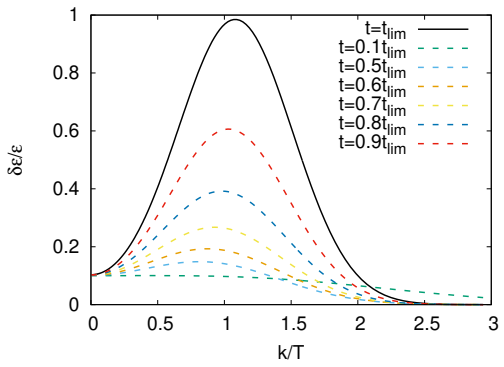

FIG. 5: Perturbations energy as a function of the mode's momentum for different times.

in the de Sitter universe the value of k_* increases with time. This means that an initially stable mode with $k > k_*(0)$ may eventually enter the unstable range $0 < k < k_*$. As a result, the mode initially experiences a damping effect, causing it to decrease in amplitude. However, as time progresses the mode eventually surpasses its initial value and becomes unstable. This behavior is illustrated in FIG. 4 for a specific mode.

C. Spinodal instability in de-Sitter with variable sound speed

In the real physical case, we start by examining a state that is initially located at the spinodal point, where the sound speed is zero. Subsequently, we observe its time evolution and analyze the behavior of the sound modes as they penetrate further into the spinodal branch, leading to increasingly imaginary sound speeds. As a result, the state predominantly resides near the spinodal point for most of its time within the spinodal region. Consequently, the region around the spinodal point plays a crucial role in the phase transition of the early universe. Therefore, our study will focus on small sound velocities, where the growth of unstable modes accepts a linear analysis. In this context, the thermal time-scale is much shorter than the time-scale of variations in our system, indicating that the gradients are small enough to assume the viscosity coefficients to be constant. Close to the spinodal point, the sound speed exhibits a parabolic behavior with temperature (see FIG. 1),

$$c_s^2 = -\alpha\sqrt{\frac{T}{T_s} - 1}, \tag{12}$$

where α is a dimensionless parameter with origin in the state equation and we have assumed it to be $\alpha^2 = 1/3$. Considering that the expansion of the universe is isentropic and using the sound speed definition, we have

$$\frac{1}{T}\frac{dT}{d\epsilon} = \frac{s}{T}\frac{dT}{ds}\frac{1}{s}\frac{ds}{dt} = -3Hc_s^2. \tag{13}$$

Combining both equations, we find that the temperature close to the spinodal point satisfies

$$\frac{1}{T}\frac{dT}{dt} = 3H\alpha\sqrt{\frac{T}{T_s} - 1}. \tag{14}$$

Around the spinodal point, $t \to t_s$, we can write the solution of this equation as a power series in time. Substituting this result into eq.(12), we find that close to the spinodal point

$$c_s^2 = \frac{3}{2}H\alpha^2(t_s - t). \tag{15}$$

This assumption is only valid at regions near the spinodal point. Therefore, we will limit our calculations to a specific time, denoted as $t_{\rm lim}$, which is defined as the time when $\delta\epsilon/\epsilon(t_{\rm lim}) = 1$ for an arbitrary momentum. In other words, it is the time at which the perturbation exhibits a linear behavior. To facilitate our analysis, we will work with dimensionless variables, specifically $\delta\epsilon/\epsilon$. To do so, we perform the following variable change, $\delta\epsilon = \epsilon\delta\tilde{\epsilon}$, while keeping in mind that the background energy time dependence is $\partial_t\epsilon = -H(\epsilon + p)$ as stated previously. The behavior of the perturbations for different modes in the linear regime is shown in FIG. 5.

FIG. 5 clearly demonstrates that both k_{max} and k_* shift towards higher momenta as time elapses. We can model their specific behavior by assuming an adiabatic expansion. Indeed, in the linear regime, we can make the assumption that $Ht \to 0$. Consequently, eq.(10) becomes the same as the one found in the case of a flat universe but with a variable speed of sound. In this scenario, we can consider the expansion of the unstable modes to be adiabatic, meaning that $\delta\epsilon/\epsilon \sim e^{\tilde{\gamma}(k,t)}$, where $\tilde{\gamma}(k,t)$ represents the sum of all the Minkowski growth rates over time. This is

$$\begin{aligned}\tilde{\gamma}(k,t) &= \int_{t_s}^{t}\left[k|c_s(t')| - \frac{k^2}{2}\Gamma\right]dt' \\ &= \sqrt{\frac{2}{3}\alpha^2 H}(t-t_s)^{3/2}k - \frac{\Gamma}{2}(t-t_s)k.\end{aligned} \tag{16}$$

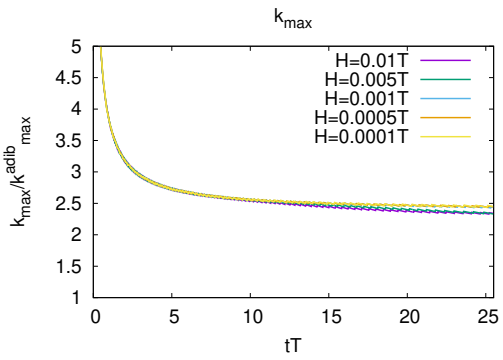

FIG. 6: k_{max}/k^{adib}_{max} as a time function for different values of the Hubble's parameter in the linear regime.

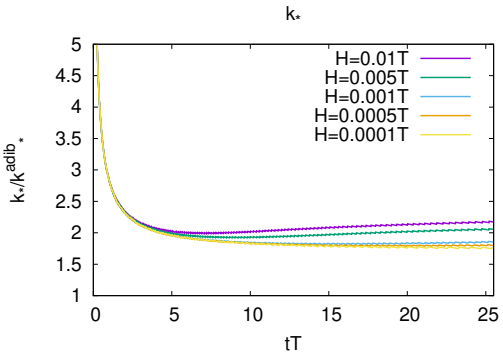

FIG. 7: k_*/k^{adib}_* as a time function for different values of the Hubble's parameter in the linear regime.

Hence the most unstable and threshold modes are

$$k^{adib}_{max} = \sqrt{2\alpha^2 H(t-t_s)/3\Gamma^2} \quad k^{adib}_* = 2k^{adib}_{max}. \qquad (17)$$

In FIG. 6 and 7 we have presented the results for different values of H. Eq.(17) tells that for larger values of H, both k_{max} and k_* move to larger momenta more rapidly. To ensure that the behavior of the modes in the linear regime is independent of the magnitude of the universe expansion, we have illustrated their quotient with their adiabatic counterparts. It is interesting to observe that the most unstable and threshold mode computed stabilize at values $k_{max} \approx 2.4k^{adib}_{max}$ and $k_* \approx 2k^{adib}_*$.

It is important to mention that the adiabatic approximation is only effective in describing the momentum of the most unstable and threshold modes, but it does not accurately describe the amplitude of the unstable modes.

IV. CONCLUSIONS

This study investigates the behavior of states in the spinodal region within an expanding universe, with a particular focus on the dynamics of sound modes during the phase transition of the early universe.

Considering small perturbations in energy density and fluid velocity we have determined a differential equation for energy fluctuations. By analyzing the system's behavior as it progresses deeper into the spinodal branch, we have gained valuable insights into the characteristics of unstable modes. Specifically, we have determined that the spinodal instability exhibits an infrared nature, with only modes of lower momenta being susceptible to instability. Furthermore, we have obtained the time evolution of both the most unstable mode and the threshold mode. Notably, near the spinodal point, we can model both k_{max} and k_* by assuming that the unstable modes exhibit an adiabatic expansion, resulting in $k_{max} \approx 2.4k^{adib}_{max}$ and $k_* \approx 2k^{adib}_*$ regardless of the value of H.

In summary, this research provides insights into the dynamics of sound modes in the spinodal region of an expanding universe. A further non-linear analysis of the system using hydrodynamics beyond the linearized approximation should be performed to fully understand how the early universe phase transition occurred.

Acknowledgments

I would like to acknowledge my advisor, Dr. Casalderrey, for their guidance and support, as well as my family for their unwavering encouragement.

[1] Mark Hindmarsh and Marvin Lüben and Johannes Lumma and Martin Pauly. "Phase transitions in the early universe". SciPost Physics Lecture Notes (2021).

[2] Bea, Yago and Casalderrey-Solana, Jorge and Giannakopoulos, Thanasis and Jansen, Aron and Krippendorf, Sven and Mateos, David and Sanchez-Garitaonandia, Mikel and Zilhão, Miguel. "Spinodal Gravitational Waves". (2021). 2112.15478.

[3] Attems, Maximilian and Bea, Yago and Casalderrey-Solana, Jorge and Mateos, David and Zilhão, Miguel. "Dynamics of Phase Separation from Holography ". JHEP **01**: 106 (2020).

[4] Paul Romatschke. "NEW DEVELOPMENTS IN RELATIVISTIC VISCOUS HYDRODYNAMICS". World Scientific Pub Co Pte Lt **19**: 1-53 (2010).

[5] Paul Romatschke. "Relativistic viscous fluid dynamics and non-equilibrium entropy". Classical and Quantum Gravity **27**: 025006 (2009).

[6] Paul Romatschke and Ulrike Romatschke. "Relativistic Fluid Dynamics In and Out of Equilibrium – Ten Years of Progress in Theory and Numerical Simulations of Nuclear Collisions". (2019). 1712.05815.

[7] Kovtun, P. K. and Son, D. T. and Starinets, A. O.. "Viscosity in Strongly Interacting Quantum Field Theories from Black Hole Physics". Phys. Rev. Lett. **94**: 111601 (2005).

Appendix A: Viscous-stress tensor perturbations

In this section a detailed proof of eq.(5) is provided. The viscous-stress tensor can be written as an expansion of gradients using all the symmetric traceless tensors and scalars that can be form independently. Up to second order one has

$$\begin{aligned}
\Pi^{\mu\nu} &= \pi^{\mu\nu} + \Delta^{\mu\nu}\Pi. \\
\pi^{\mu\nu} &= -\eta\sigma^{\mu\nu} + \eta\tau_\pi D\sigma^{<\mu\nu>} + \eta\tau_\pi^*\frac{\nabla_\alpha u^\alpha}{3}\sigma^{\mu\nu} \\
&\quad + \kappa R^{<\mu\nu>} + \kappa^* 2u_\alpha u_\beta R^{\alpha<\mu\nu>\beta} \\
&\quad + \lambda_1\sigma_\lambda^{<\mu}\sigma^{\nu>\lambda} + \lambda_2\sigma_\lambda^{<\mu}\Omega^{\mu>\lambda} \\
&\quad + \lambda_3\Omega_\lambda^{<\mu}\Omega^{\nu>\lambda} + \lambda_4\nabla^{<\mu}\ln s\nabla^{\nu>}\ln s \\
\Pi &= -\zeta(\nabla_\alpha u^\alpha) + \zeta\tau_\Pi(\nabla_\alpha u^\alpha) + \xi_1\sigma^{\mu\nu}\sigma_{\mu\nu} \\
&\quad + \xi_2(\nabla_\alpha u^\alpha)^2 + \xi_3\Omega^{\mu\nu}\Omega_{\mu\nu} \\
&\quad + \xi_4\nabla_\mu^\perp\ln s\nabla_\perp^\mu\ln s + \xi_5 R + \xi_6 u^\alpha u^\beta R_{\alpha\beta}.
\end{aligned} \tag{A1}$$

Let us introduce first the perturbation into the symmetric traceless part, π^{xx}:

$$\begin{aligned}
\delta\pi^{xx} &= -\eta\delta\sigma^{xx} + \eta\tau_\pi\delta(D\sigma^{xx}) + \eta\tau_\pi^*\delta\left(\frac{\nabla_\alpha u^\alpha}{3}\sigma^{xx}\right) \\
&\quad + \kappa\delta R^{<xx>} + \kappa^* 2\delta(u_\alpha u_\beta R^{\alpha<xx>\beta}).
\end{aligned} \tag{A2}$$

The other terms vanish when introducing the perturbations since they will always have spatial derivatives of the velocity or energy density of the background and are, hence, null. The terms in eq.(A2) are then computed individually. The resulting expressions are

$$\begin{aligned}
-\eta\delta\sigma^{xx} &= -\eta\left[2\nabla_\perp^{(x}\delta u^{x)} - \frac{2}{3}g^{xx}\nabla_x\delta u^x\right] \\
&= -\frac{4}{3}\eta e^{-2Ht}\partial_x\delta u^x
\end{aligned}$$

$$\begin{aligned}
\eta\tau_\pi\delta(D\sigma^{xx}) &= \eta\tau_\pi(\delta D)\sigma^{xx} + \eta\tau_\pi D\delta\sigma^{xx} \\
&= +\frac{4}{3}\tau_\pi\eta e^{-2Ht}\partial_t\partial_x\delta u^x
\end{aligned}$$

$$\begin{aligned}
\eta\tau_\pi^*\delta\left(\frac{\nabla_\alpha u^\alpha}{3}\sigma^{xx}\right) &= \eta\tau_\pi^*\left[\delta\left(\frac{\nabla_\alpha u^\alpha}{3}\right)\sigma^{xx} + \frac{\nabla_\alpha u^\alpha}{3}\delta\sigma^{xx}\right] \\
&= \frac{4}{3}\eta e^{-2Ht}\frac{\tau_\pi^*}{3}H\partial_x\delta u^x.
\end{aligned}$$

To compute the fourth one, we notice $R_{xx} = \partial_\lambda\Gamma^\lambda_{xx} - \partial_x\Gamma^\lambda_{x\lambda} + \Gamma^\rho_{xx}\Gamma^\lambda_{\rho\lambda} - \Gamma^\rho_{\lambda\lambda}\Gamma^\lambda_{\rho x} = \partial_0\Gamma^0_{xx} - \Gamma^x_{x0}\Gamma^0_{xx} = Hg_{xx}$. Therefore $\delta R^{<xx>} \sim \delta g^{xx} = 0$. Finally the fifth term reads

$$\begin{aligned}
\delta(u_\alpha u_\beta R^{\alpha<xx>\beta}) &= \delta(u_\alpha u_\beta)R^{\alpha<xx>\beta} + u_\alpha u_\beta\delta R^{\alpha<xx>\beta} \\
&= 0.
\end{aligned}$$

In the expression above, the first part becomes zero because $R^x_{xx0} = R^0xxx = 0$ and it only remains when either $\alpha = x$ and $\beta = 0$, or vice versa. Consequently, $R^{\alpha<xx>\beta} = 0$. The second part disappears because it only persists when $\alpha = \beta = 0$, and in that case, $R^0xx0 = -Hg_{xx}$. Hence, we have $\delta R^{\alpha<xx>\beta} \approx \delta g^{xx} = 0$.

When perturbing the trace part of the viscous tensor, the following terms are the only ones that remain non-zero,

$$\begin{aligned}
\delta\Pi &= -\zeta\delta(\nabla_\alpha u^\alpha) + \zeta\tau_\Pi\delta(D\nabla_\alpha u^\alpha) \\
&\quad + \xi_2\delta\left(\nabla_\alpha u^\alpha\right)^2 + \xi_5\delta R + \xi_6\delta(u_\alpha u_\beta R^{\alpha\beta}).
\end{aligned} \tag{A3}$$

Again, we compute $\delta\Pi$ term by term. The first three read

$$-\zeta\nabla_\alpha\delta u^\alpha = -\zeta\nabla_x\delta u^x = -\zeta\partial_x\delta u^x$$

$$\zeta\tau_\Pi\delta(D\nabla_\alpha u^\alpha) = \zeta\tau_\Pi(\delta D\nabla_\alpha u^\alpha + D\nabla_\alpha\delta u^\alpha) = \zeta\tau_\Pi\partial_t\partial_x\delta u^x$$

$$\xi_2\delta\left(\nabla_\alpha u^\alpha\right)^2 = 2\xi_2\nabla_\alpha u^\alpha(\nabla_\alpha\delta u^\alpha) = 2\zeta\tau_\Pi^* H\partial_x\delta u^x$$

where we have used that $\nabla_x\delta u^i = \partial_x\delta u^i$ and have defined $\xi_2 \equiv \zeta\tau_\Pi^*$. The fourth term is null since we suppose that the perturbations don't act in the metrics, hence neither in the curvature. The fifth term can be expressed in two parts: $\delta(u^\alpha u^\beta)R_{\alpha\beta} + u^\alpha u^\beta\delta R_{\alpha\beta}$. The first one is zero because $R_{x0} = R_{0x} = 0$ and the second one vanishes since we suppose $\delta g_{\alpha\beta} = 0$.

Finally introducing the computed terms of eq.(A2) and (A3) into eq.(A1), one finds that the perturbation of the general stress-tensor reads

$$\begin{aligned}
\delta\Pi^{xx} &= \delta\pi^{xx} + e^{-2Ht}\delta\Pi \\
&= -\left[\frac{4}{3}\eta\left(1 - \frac{\tau_\pi^*}{3}H\right) + \zeta(1 - 2\tau_\Pi^* H)\right]e^{-2Ht}\partial_x\delta u^x \\
&\quad + \left(\frac{4}{3}\eta\tau_\pi + \zeta\tau_\Pi\right)e^{-2Ht}\partial_x\partial_t\delta u^x.
\end{aligned} \tag{A4}$$

In the second part of the last equation, one can substitute the time derivative of the velocity with a spatial derivative of the energy density. Indeed, differentiating the relativistic Navier-Stokes equation for the perturbations (bottom eqs.(4)) with respect to the spatial coordinate x, one finds

$$\partial_x\partial_t\delta u^x = -\frac{c_s^2}{\epsilon + p}e^{-2Ht}\partial_x^2\delta\epsilon - H\partial_x\delta u^x + \mathcal{O}(\partial^3\dots).$$

Here the higher order in gradients terms come from the viscous stress tensor part. With this, $\delta\Pi^{xx}$ can be written as

$$\begin{aligned}
\delta\Pi^{xx} &= -\frac{4}{3}\eta\left[1 + \left(\tau_\pi - \frac{\tau_\pi^*}{3}\right)H\right]e^{-2Ht}\partial_x\delta u^x \\
&\quad + \zeta\left[1 + \left(\tau_\Pi - 2\tau_\Pi^*\right)H\right]e^{-2Ht}\partial_x\delta u^x \\
&\quad - \frac{c_s^2}{\epsilon + p}\left(\frac{4}{3}\eta\tau_\pi + \zeta\tau_\Pi\right)e^{-4Ht}\partial^2\delta\epsilon
\end{aligned}$$

This equation takes the same form as the one previously introduced (eq.(5)) if we define a sound attenuation in de Sitter space and identify the longitudinal transport coefficient as given by eq.(6) and (7).